

## SHAPING THE RADIATION PATTERN WITH MU AND EPSILON-NEAR-ZERO METAMATERIALS

**B. Wang and K.-M. Huang**

College of Electronics and Information Engineering  
Sichuan University  
Chengdu, Sichuan 610065, China

**Abstract**—In this paper, mu and epsilon-near-zero (MENZ) metamaterials are used to convert the waves emitted from an embedded line source to various waveforms. The simulation results show that the converted waveforms are consistent with the exit face shape of the metamaterials. The power distributions in different beams are dependent on the length proportion of the exit faces due to its impedance matching with the surrounding media, which is different from the epsilon-near-zero (ENZ) metamaterials. A numerical verification with the finite element method (FEM) was presented, followed by physical insights into this phenomenon and theoretical analysis. We also propose some potential applications, including high directive emissions, multi-beams emissions.

### 1. INTRODUCTION

In recent years, metamaterials have attracted substantial interest. Many attractive properties due to their extraordinary effective parameter of permittivity  $\epsilon$  or permeability  $\mu$  have been analyzed [1], and some potential applications have been explored, including negative index of refraction [2–5], perfect lenses which can break the usual wavelength limits with double negative index materials [6], EM concentrators [7], subwavelength waveguides [8, 9], electromagnetic wave rotators [10], and cloaking devices [11–17], etc. Limits that were considered insurmountable in conventional setups have indeed been shown to be, at least potentially, surpassed when the special materials are employed [18].

In many studies on metamaterials, one of the main attempts has been to manipulate radiation beams or wave behavior to form a desired field distribution. Alù and co-researchers studied the possibility of using various geometries  $\epsilon$ -near-zero (ENZ) materials to tailor the phase pattern [18]. Ziolkowski discussed the propagation and scattering of microwave in cylinder and sphere shape  $\mu$  and epsilon-near-zero metamaterials with the FDTD method [19]. Since Enoch et al. proposed the scheme of directive emission by embedding a source in an ENZ metamaterial slab in 2002 [20], several attempts have been presented with analogous purposes [11–27]. Recently, high directive emissions [28, 29] and multi-beams [30, 31] have been achieved with the transformation optics technique, which provides a great opportunity for designing novel electromagnetic and optical devices. However, applications of the transformation optics technique have typically led to highly anisotropic and inhomogeneous solutions for the required permittivity and permeability of a device, making constitutive parameters too complex to implement practically in current fabrication techniques.

In this paper, we present a scheme of manipulating radiation beams to form a desired field distribution with MENZ metamaterials, which is more feasible than metamaterials obtained from the transformation optics technique. By embedding sources inside metamaterials with special exit face shape, the emitted waveforms can be converted into a desired form, and power allocations in different beams with any proportion can be realized. The differences between our work and the strategy of Alù et al. [18] lie in the problems of the impedance mismatch between the ENZ metamaterials and surrounding media. The MENZ metamaterials adopted here have the same value of relative permittivity and relative permeability approaching zero, allowing them to match the surrounding air. There is no reflection at the boundaries, and a real uniform distribution of electric intensity is achieved inside the medium, endowing them with the capacity of exact control of the radiation shape and power allocation in different beams. This effect may be employed and play an important role in wireless communications and radar technology. The basic mechanism on the phenomenon is analyzed, and numerical verifications with the finite element method (FEM) are presented. We also propose some potential applications, including high directive emissions, multi-beams emissions.

## 2. HEURISTIC ANALYSIS

When the electromagnetic field is excited from a line current source, considering a medium with the same value of relative permittivity and relative permeability approaching zero, the Maxwell's equations can be reduced to

$$\nabla \times \vec{E} = 0 \quad \nabla \times \vec{H} = \vec{J} \quad \nabla \cdot (\varepsilon_0 \varepsilon_r \vec{E}) = 0 \quad \nabla \cdot (\mu_0 \mu_r \vec{H}) = 0 \quad (1)$$

where  $\vec{J}$  is the current density. The electromagnetic field behaves as a combination of a constant electric field and a magnetostatic magnetic field. The specific values depend on the source and MENZ metamaterials configuration. When the configuration is complex, it is not easy to give an exact analytical solution. However, the electric distribution inside MENZ metamaterials will keep uniform when the shape changes. Considering the refractive index of MENZ metamaterials  $n = \sqrt{\varepsilon_r \mu_r}$  is approaching zero, the wave from any direction will be turned to the norm of the interface. Putting these two consequences together plus the boundary conditions that the tangential components of the electric and magnetic field must be continuous at the boundaries, the distribution of electric field along the interface is uniform. In another word, the emitted waveforms will be consistent with the exit face of the metamaterials as shown in Figure 1, and the power outflow proportions in different beams are dependent on the lengths of the interfaces.

Isotropic metamaterials design has been an important research topic in recent years. Several groups have studied isotropic metamaterials with low or negative permittivity or permeability analytically and experimentally [32–37]. Therefore, we justifiably limit our simulations to isotropic metamaterials with negligible spatial dispersion, which represent a wide class of available natural plasmonic materials and several types of metamaterials [18]. Considering the polarization of the line current source used in our scheme, the propagation and scattering of the emitted wave will be affected by  $\varepsilon_{rz}$ ,  $\mu_{rx}$  and  $\mu_{ry}$  in the coordinates shown in Figure 2. So metamaterials with permittivity near zero in the  $z$  direction and isotropic permittivity in  $x$ - $y$  plane are needed in a practical application.

## 3. THE SIMULATION MODEL

The simulation model is shown in Figure 2, and a  $z$ -axis oriented line current valued as  $\vec{I} = \vec{e}_z \exp(i\omega t)$  is employed as a source, where  $\omega$  is the angular frequency. It is placed in the center of the calculation

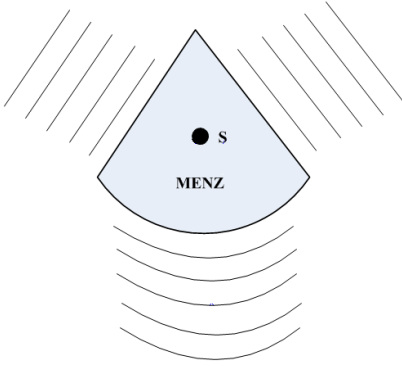


**Figure 1.** The waveforms are converted to consistent with the exit face.

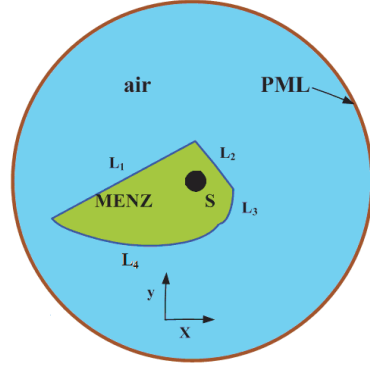


**Figure 2.** The simulation model.

**Table 1.** Scales of the boundaries.

	$L_1$	$L_2$	$L_3$	$L_4$	Total
Length (m)	0.81	0.36	0.35	0.91	2.43
Proportion	33.33%	14.82%	14.40%	37.45%	100%

area and embedded in arbitrary shaped MENZ metamaterials, whose borders are composed of four curves  $L_1$ ,  $L_2$ ,  $L_3$  and  $L_4$ .  $L_1$ ,  $L_2$  are set as straight lines, and  $L_3$ ,  $L_4$  are set as curves with different curvatures here. Their lengths and proportions in the total length are shown in Table 1. The MENZ metamaterials are surrounded by air. The boundaries of the calculation area are surrounded by perfect impedance matching layers (PML). Considering the losses in metamaterials, we set the constitutive parameters as  $\epsilon_r = 10^{-7} - 0.05i$ ,  $\mu_r = 10^{-7} - 0.005i$  and did the simulation at 3 GHz.

#### 4. THE CALCULATION RESULTS AND ANALYSIS

Waves have low-wave-number indexes near zero in MENZ metamaterials, which provides a relatively small phase variation in the medium. When waves interface with air, an uniform phase distribution inside the metamaterials will be produced as shown in Figure 3. Outside the metamaterials, the phase front is consistent with the exit face shape. Waves are separated into four main beams: Plane-wave-like emissions are obtained at the straight border  $L_1$  and  $L_2$ ; curve emissions are achieved at the border  $L_3$  and  $L_4$ . When the ellipse-like and sector

shape MENZ metamaterials are employed, a similar phenomenon is observed as shown in Figure 4 and Figure 5, respectively. Based on these properties, we can transform the phase distribution from a line source into a desired shape by properly tailoring the exit side of the MENZ slab.

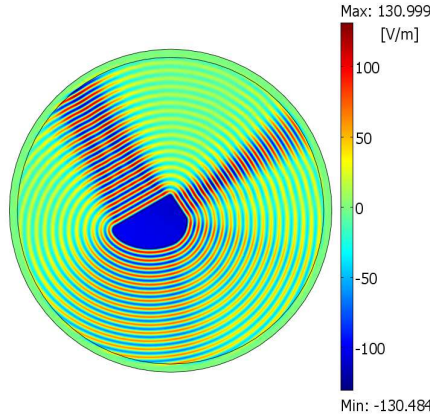


Figure 3. The electric field distributions.

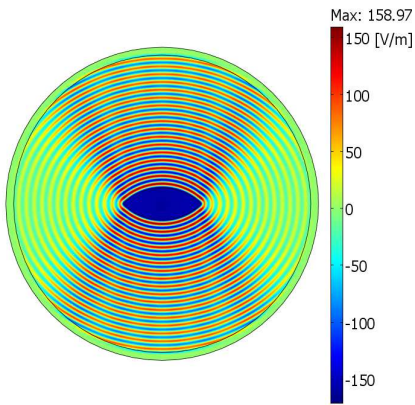


Figure 4. The electric field distributions with the shape ellipse-like shaped metamaterials.

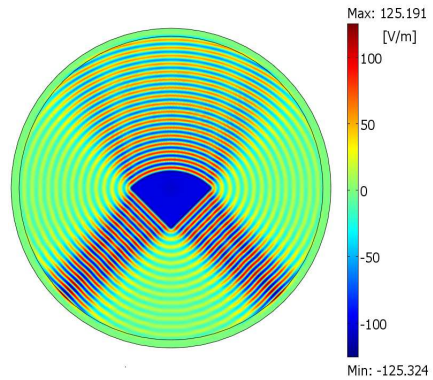
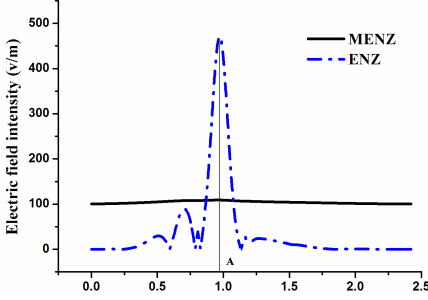
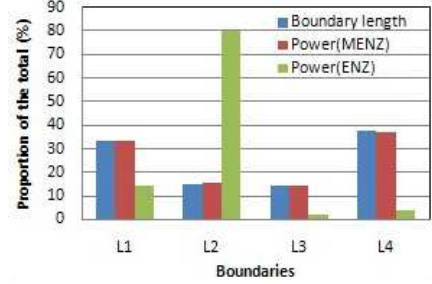


Figure 5. The electric field distributions with the sector shaped metamaterials.

Next, we focused on the power allocation ability of MENZ metamaterials. We investigated the electric intensity distribution and



**Figure 6.** The Electric intensity at different positions of the boundary.



**Figure 7.** The proportions of the boundary length and the average power outflow.

power outflows at the boundaries  $L_1$ ,  $L_2$ ,  $L_3$  and  $L_4$ . The same shaped epsilon-near-zero metamaterial slab, whose constitutive parameters were set as  $\varepsilon_r = 10^{-7} - 0.05i$  and  $\mu_r = 1$ , was also employed for a comparative study.

Figure 6 shows the electric intensity distributions at different positions of the boundary with ENZ and MENZ metamaterials, where the  $x$ -axis coordinate represents the length of the border from a certain point to the left end of  $L_1$  along the counterclockwise direction. The electric intensity distribution is almost uniform at the boundaries between the MENZ metamaterials and air. But it is obviously irregular and has a larger value at point  $A$ , which is on  $L_2$  when ENZ metamaterials are employed.

Figure 7 shows the relationships between the boundary length and the average power outflows. The proportion of power outflows is independent of the length proportion of the boundaries when ENZ metamaterials are employed. The largest proportion of power outflow is assigned to  $L_2$ , which is closer to the source. However, the proportions of the power outflow at each boundary are equal to that of the boundary lengths when MENZ metamaterials are employed, which implies that a line source with MENZ metamaterials has the capability of emitting power with desired proportions in different directions and different waveforms. So we can conclude that the radiation from a line source can be shaped into a desired pattern, and multi-beams power allocation is achieved simultaneously with the MENZ metamaterials.

## 5. APPLICATIONS

By controlling the shape and length of the interfaces of the mu and epsilon-near-zero metamaterials, it is possible to engineer the phase radiation pattern arbitrarily, forming a planar wavefront or a convergent cylindrical wavefront with different power proportions. These effects may have interesting applications in several fields, such as high directive emissions and multi-beams emissions with a desired power proportion.

### 5.1. High Directive Emissions

High directive emissions with metamaterials have attracted much attention in recent years [18–29], some of which are achieved with the transformation optics technique. Here, we will demonstrate how the mu and epsilon-near-zero metamaterials can be adopted to form a high directive emission.

As shown in Figure 8, a rectangular MENZ metamaterial slab with an aspect ratio  $k = L/H$  is employed to achieve a high directive emission, where  $L$  is the length of the slab, and  $H$  is the thickness. Considering the refractive index of MENZ metamaterials  $n = \sqrt{\epsilon_r \mu_r}$  is close to zero, waves from any directions will be turned into the norm of the boundary. As mentioned above, the power outflow in different directions are decided by the proportions of the exit face lengths. When the slab is thin enough (with a relative large value of  $k$ ) and has planar faces, high directive emission can be expected.

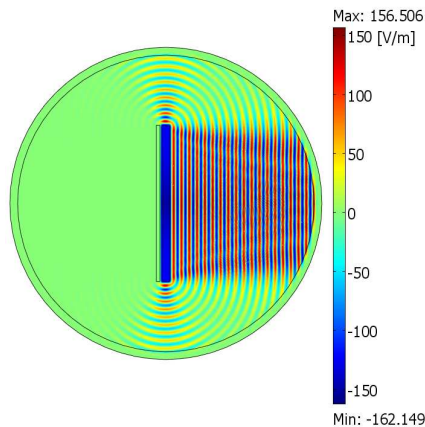


**Figure 8.** The electric field distributions of a high directive emission.

Here, we set the dimension of the slab as  $\lambda_0 \times 20\lambda_0$  ( $k = 20$ ), where  $\lambda_0$  is the wavelength in air. In order to emit the power into only one direction, we set a plan metal reflector  $\lambda_0/4$  behind it, making the phase difference between the reflected wave from the metal slab and emitted wave from the source equal to  $2\pi$  and achieving a high efficiency combining electric field. The ultra high directivity of the line antenna embedded in the MENZ metamaterials with different  $k$  is shown in Figures 9(a) and (b). When  $k$  is larger, the directivity will increase, and the side lobes will become lower. This plane-like-wave emission can also be ascribed to the uniform electric distribution at the exit face of the slab.

## 5.2. Multi-beams Power Allocation

Multi-beams emission plays an important role in wireless communications and radar technology. It is usually achieved with complex phased arrays. With the progresses in metamaterial researches, it is possible to steer multi-beams when this medium is employed. Ref. [30] has presented a scheme to form multi-beams with metamaterials through transformation optics technique. However, the constitutive parameters of the medium used in their scheme are too complex to realize. And the antenna in their scheme can only emit the same power toward each direction. Here, we will demonstrate a feasible way to realize arbitrary multi-beam power allocation with any proportion.

Firstly, we will realize a desired six-beams plane wave emission whose proportion of power outflow is  $1 : 1 : 1 : 1 : 1 : 1$ . As the

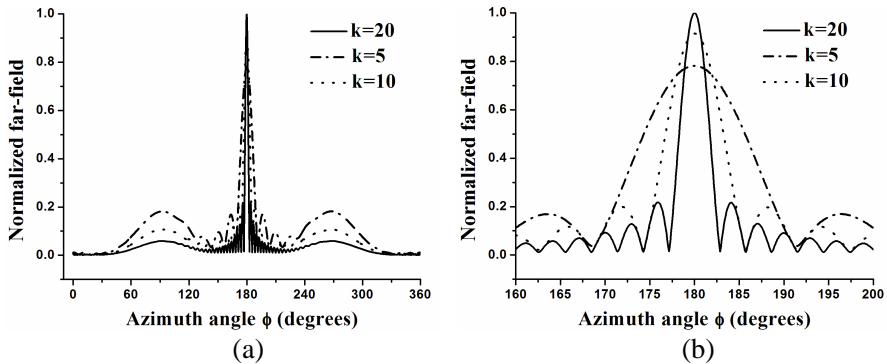


**Figure 9.** The normalized far-field distributions of a high directive emission. All curves are normalized to the far-field intensity when  $k = 20$ . (a) Full description. (b) Local description.

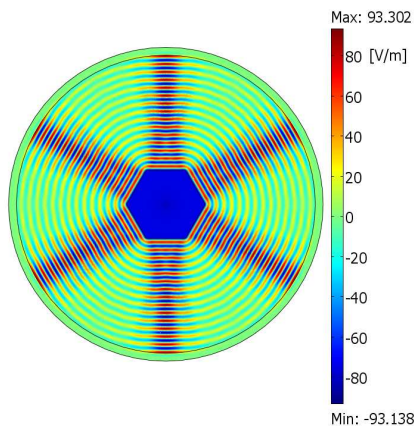


**Figure 10.** The electric field distributions of a six-beams emission.

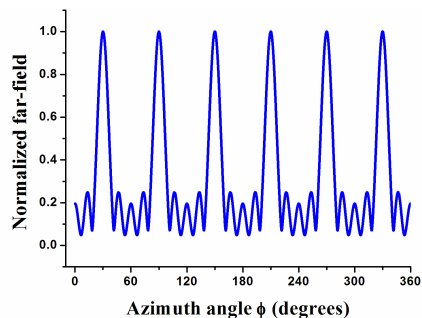


**Figure 11.** The normalized far-field.

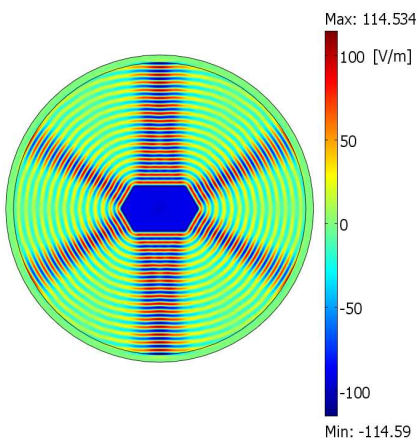


**Figure 12.** The electric field distributions of a six-beams emission.

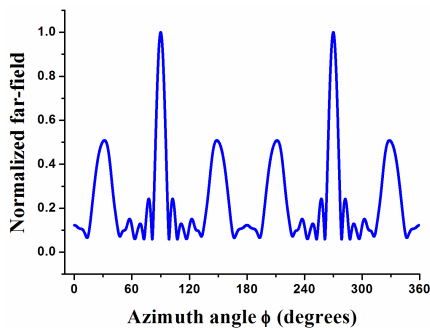


**Figure 13.** The normalized far-field.

proportion of the power outflow is dependent on the relative length of each boundary, a regular hexagon shape MENZ metamaterials should be adopted. Figure 10 describes the amplitude of the emitted electric field distribution. The transverse-electric (TE) cylindrical wave emitted from the line current source is evenly separated into six-beams plane waves. Figure 11 shows the far field radiation directivities. The directivities in six directions are relatively high and almost the same,

which implies the power outflow from each boundary is equal to each other.

As shown in Figure 12 and Figure 13, when the proportion of the boundaries becomes 1 : 2 : 1 : 1 : 2 : 1, the electric field intensity in six directions will still keep uniform but the proportion of the power outflow becomes 1 : 2 : 1 : 1 : 2 : 1. In fact, based on the properties of  $\mu$  and epsilon-near-zero metamaterials discussed in part three, other more complex shape and proportion of power outflow emissions can be rationally expected.

## 6. CONCLUSION

In this paper,  $\mu$  and epsilon-near-zero metamaterials are used to shape the radiation pattern of an embedded line source. Theoretical analysis followed by a numerical verification with the finite element method (FEM) is presented. The simulation results show that the converted waveforms are consistent with the exit face shapes of the metamaterials. The power distributions are decided by the relative length of the exit faces due to the MENZ metamaterials' impedance matching with the surrounding air. Based on these properties, arbitrary shape emission with any desired proportion of power outflow can be realized. High directive emissions and multi-beams power allocations are also considered as potential applications for this medium.

## REFERENCES

1. Tretyakov, S., I. Nefedov, A. Sihvola, S. Maslovski, and C. Simovski, "Waves and energy in chiral nihility," *Journal of Electromagnetic Waves and Applications*, Vol. 17, No. 5, 695–706, 2003.
2. Smith, D. R., J. B. Pendry, and M. C. K. Wiltshire, "Metamaterials and negative refractive index," *Science*, Vol. 305, 788, 2004.
3. Lepetit, T., É. Akmansoy, and J. P. Ganne, "Experimental measurement of negative index in an all-dielectric metamaterial," *Appl. Phys. Lett.*, Vol. 95, 2009.
4. Shelby, R. A., D. R. Smith, and S. Schultz, "Experimental verification of a negative index of refraction," *Science*, Vol. 292, 77, 2001.
5. Akhlesh, L., "An electromagnetic trinity from negative permittiv-

- ity and negative permeability,” *International Journal of Infrared and Millimeter Waves*, Vol. 23, No. 6, 2002.
6. Pendry, J. B., “Negative refraction makes a perfect lens,” *Phys. Rev. Lett.*, Vol. 85, No. 18, 3966–3969, 2000.
  7. Jiang, W. X., T. J. Cui, Q. Cheng, J. Y. Chin, X. M. Yang, R. Liu, and D. R. Smith, “Design of arbitrarily shaped concentrators based on conformally optical transformation of nonuniform rational B-spline surfaces,” *Appl. Phys. Lett.*, Vol. 92, No. 26, 2008.
  8. Silveirinha, M. and N. Engheta, “Tunneling of electromagnetic energy through subwavelength channels and bends using  $\epsilon$ -near-zero materials,” *Phys. Rev. Lett.*, Vol. 97, 157403, 2006.
  9. Tassin, P., X. Sahyoun, and V. Veretennicoff, “Miniaturization of photonic waveguides by the use of left-handed materials,” *Appl. Phys. Lett.*, Vol. 92, 203111, 2008.
  10. Chen, H. and C. T. Chan, “Transformation media that rotate electromagnetic fields,” *Appl. Phys. Lett.*, Vol. 90, No. 24, 2007.
  11. Pendry, J. B., D. Schurig, and D. R. Smith, “Controlling electromagnetic fields,” *Science*, Vol. 312, No. 5781, 1780–1782, 2006.
  12. Cheng, X., H. Chen, X. M. Zhang, B. Zhang, and B. I. Wu, “Cloaking a perfectly conducting sphere with rotationally uniaxial nihility media in monostatic radar system,” *Progress In Electromagnetics Research*, Vol. 100, 285–298, 2010.
  13. Starr, A. F. and D. R. Smith, “Metamaterial electromagnetic cloak at microwave frequencies,” *Science*, Vol. 314, 2006.
  14. Leonhardt, U., “Optical conformal mapping,” *Science*, Vol. 312, No. 5781, 1777–1780, 2006.
  15. Cheng, Q., W. X. Jiang, and T. J. Cui, “Investigations of the electromagnetic properties of three-dimensional arbitrarily-shaped cloaks,” *Progress In Electromagnetics Research*, Vol. 94, 105–117, 2008.
  16. Zhang, J. J., Y. Luo, H. Chen, and B. I. Wu, “Sensitivity of transformation cloak in engineering,” *Progress In Electromagnetics Research*, Vol. 84, 93–104, 2008.
  17. Vafi, K., A. Javan, and M. Abrishamian, “Dispersive behavior of plasmonic and metamaterial coating on achieving transparency,” *Journal of Electromagnetic Waves and Applications*, Vol. 22, No. 7, 941–952, 2008.
  18. Alù, A., M. G. Silveirinha, A. Salandrino, and N. Engheta, “Epsilon-near-zero metamaterials and electromagnetic sources:

- Tailoring the radiation phase pattern,” *Phys. Rev. B*, Vol. 75, No. 15, 2007.
19. Ziolkowski, R. W., “Propagation in and scattering from a matched metamaterial having a zero index of refraction,” *Phys. Rev. E*, Vol. 70, 2004.
  20. Enoch, S., G. Tayeb, P. Sabouroux, N. Guerin, and P. Vincent, “A metamaterial for directive emission,” *Phys. Rev. Lett.*, Vol. 89, No. 21, 213902, 2002.
  21. Yu, Y., L. F. Shen, L. X. Ran, T. Jiang, and J. T. Huangfu, “Directive emission based on anisotropic metamaterials,” *Phys. Rev. A*, Vol. 77, 2008.
  22. Wu, Q., P. Pan, F. Y. L. Meng, W. Li, and J. Wu, “A novel flat lens horn antenna designed based on zero refraction principle of metamaterials,” *Appl. Phys. A.*, Vol. 87, 151–156, 2007.
  23. Zhou, H., Z. Pei, S. Qu, S. Zhang, J. Wang, Q. Li, and Z. Xu, “A planar zero-index metamaterial for directive emission,” *Journal of Electromagnetic Waves and Applications*, Vol. 23, No. 7, 953–962, 2009.
  24. Yang, J. J., M. Huang, and J. H. Peng, “Directive emission obtained by  $\mu$  and  $\epsilon$ -near-zero metamaterials,” *Radio Engineering*, Vol. 18, 2009.
  25. Weng, Z. B., X. M. Wang, and Y. Song, “A directive patch antenna with arbitrary ring aperture lattice metamaterial structure,” *Journal of Electromagnetic Waves and Applications*, Vol. 23, No. 13, 1763–1772, 2009.
  26. Zhou, H., Z. Pei, and S. Qu, “A planar zero-index metamaterial for directive emission,” *Journal of Electromagnetic Waves and Applications*, Vol. 23, No. 7, 953–962, 2009.
  27. Weng, Z. B., Y. C. Jiao, G. Zhao, and F. S. Zhang, “Design and experiment of one dimension and two dimension metamaterial structures for directive emission,” *Progress In Electromagnetics Research*, Vol. 70, 199–209, 2007.
  28. Zhang, J., Y. Luo, H. Chen, L. Ran, B. I. Wu, and J. A. Kong, “Directive emission obtained by coordinate transformation,” *Progress In Electromagnetics Research*, Vol. 81, 2008.
  29. Kong, F., B. I. Wu, J. A. Kong, J. Huangfu, S. Xi, and H. Chen, “Planar focusing antenna design by using coordinate transformation technology,” *Appl. Phys. Lett.*, Vol. 91, 2007.
  30. Yang, Y., X. Zhao, and T. Wang, “Design of arbitrarily controlled multi-beam antennas via optical transformation,” *J. Infrared Milli Terahz Waves*, Vol. 30, 337–348, 2009.

31. Turpin, J. P., A. T. Massoud, Z. H. Jiang, P. L. Werner, and D. H. Werner, "Conformal mappings to achieve simple material parameters for transformation optics devices," *Optics Express*, Vol. 18, No. 1, 2010.
32. Vendik, I. B., M. A. Odit, and D. S. Kozlov, "3D isotropic metamaterial based on a regular array of resonant dielectric spherical inclusions," *Metamaterials*, Vol. 3, 140–147, 2009.
33. Anthony, G. and V. E. George, "Isotropic three-dimensional negative-index transmission-line metamaterial," *Journal of Applied Physics*, Vol. 98, 043106, 2005.
34. Baena, J. D., "Electrically small isotropic three-dimensional magnetic resonators for metamaterial design," *Appl. Phys. Lett.*, Vol. 88, 2006.
35. Shelby, R. A., D. R. Smith, S. C. Nemat-Nasser, and S. Schultz, "Microwave transmission through a two-dimensional, isotropic, left-handed metamaterial," *Appl. Phys. Lett.*, Vol. 74, No. 4, 2001.
36. Koschny, T., L. Zhang, and C. M. Soukoulis, "Isotropic three-dimensional left-handed metamaterials," *Physical Review B*, Vol. 71, 2005.
37. Matra, K. and N. Wongkasem, "Left-handed chiral isotropic metamaterials: Analysis and detailed numerical study," *Journal of Optics A: Pure and Applied Optics*, Vol. 11, 2009.